Inorganica Chimica Acta 366 (2011) 85–90

Contents lists available at ScienceDirect

Inorganica Chimica Acta

journal homepage: www.elsevier.com/locate/ica

Coordinated nitroxyl anion is produced and released as nitrous oxide by the decomposition of iridium-coordinated nitrosothiols

Daniel Kazhdan [a], Laura L. Perissinotti [a], Bernardo Watanabe [a], Marcos N. Eberlin [b], Humberto M.S. Milagre [b], Boniek G. Vaz [b], Dario A. Estrin [a], Fabio Doctorovich [a,*]

[a] Departamento de Química Inorgánica, Analitica y Química Física/INQUIMAE-CONICET, Facultad de Ciencias Exactas y Naturales, Universidad de Buenos Aires, Ciudad Universitaria, Pabellón II, C1428EHA Buenos Aires, Argentina
[b] ThoMSon Mass Spectrometry Laboratory, Institute of Chemistry, State University of Campinas, UNICAMP, CEP 13083-970, C.P. 6154, Campinas SP, Brazil

ARTICLE INFO

Article history:
Received 1 July 2010
Received in revised form 27 September 2010
Accepted 11 October 2010
Available online 20 October 2010

Keywords:
Iridium
Nitroxyl
Bent NO
Nitrosothiol
Decomposition
Sulfenic acid

ABSTRACT

The aqueous decomposition of the iridium coordinated nitrosothiols (RSNOs) *trans*-K[$IrCl_4(CH_3CN)$NOSPh] (**1**), and $K_2[IrCl_5(NOECyS)]$ (**2**, ECyS = cysteine ethyl ester), was studied by MS analysis of the gaseous products, ESI-MS, NMR, and UV–Vis spectroscopy. Bent NO (NO^-, nitroxyl anion), sulfenic acids and nitrite were observed as coordinated products in solution, while nitrous oxide (N_2O) and nitrogen were detected in the gas phase. The formation of coordinated NO^- and N_2O, a nitroxyl dimerization product, allows us to propose the formation of free nitroxyl (HNO) as an intermediate. Complex **1** decomposes 300 times slower than free PhSNO does. In both cases (**1** and **2**) kinetic results show a first order decomposition behavior and a very negative $\Delta S^{\neq}$, which strongly indicates an associative rate-determining step. A proposed decomposition mechanism, supported by the experimental data and DFT calculations, involves, as the first step, nucleophilic attack of H_2O on to the sulfur atom of the coordinated RSNO, producing an NO^- complex and free sulfenic acid, followed by two competing reactions: a ligand exchange reaction of this NO^- with the sulfenic acid or, to a minor extent, coordination of N_2O to produce an NO^-/N_2O complex which finally renders free N_2 and coordinated NO_2^-. Some of the produced NO^- is likely to be released from the metal center producing nitroxyl by protonation and finally N_2O by dimerization and loss of H_2O. In conclusion, the decomposition of these coordinated RSNOs occurs through a different mechanism than for the decomposition of free RSNOs. It involves the formation of sulfenic acids and coordinated NO^-, which is released from the complexes and protonated at the reaction pH producing nitroxyl (HNO), and ultimately N_2O.

1. Introduction

The decomposition of *S*-nitrosothiols (RSNOs) in water to form NO is a biologically important reaction, since it is supposed to be involved in the transport and release of NO [1]. RSNOs' stability in solution varies as a function of, among other things, the pH, oxygen, and metal content of the solution [2–4]. RSNO compounds may be prepared by treatment of the precursor thiol (RSH) with nitrosating agents [5], including nitric oxide, in the presence of electron acceptors, such as nitrosonium salts, nitrous acid, inorganic nitrites, and metal nitrosyl complexes [6]. In cases when the nitrosating agent is a metal nitrosyl, the thiol reacts with the nitrosyl ligand to form an *S*-nitrosothiol ligand coordinated to the metal center, {M–N(O)SR}. Another method that has been used to prepare nitrosothiols complexes *in situ* consists of the reaction of the free thiolate anion with the ligand NO^+ coordinated to $[Fe(CN)_5]^{3-}$ or other coordinating moieties [7,8]. Ashby and coworkers have described time-resolved IR spectra in solution for the transient "red products", the adducts that are formed when nitroprusside reacts with thiols in aqueous media [9]. This reaction of nitroprusside with thiols has been extended to a great variety of nitrosyl complexes of formula type $\{(X)_5MNO\}^n$, with X comprising ligands of different donor–acceptor abilities and M = Fe, Ru, and Os. In most cases these complexes are unstable and decompose spontaneously to metal complexes and disulfides, with the lifetimes depending strongly on the thiol structure [10].

In a previous work, we presented the reaction between a free thiol, benzyl mercaptan, and $K[IrCl_5NO]$, leading to the formation of the stable coordinated nitrosothiol *trans*-K[$IrCl_4(CH_3CN)$-N(O)SCH_2Ph] [11,12]. This was the first time that a nitrosothiol complex was isolated and fully characterized, including a structural determination by X-ray crystallography. This finding represents a good example of how the coordination chemistry of RSNOs uncovers new aspects of the nitrosation processes, since coordination to metal centers considerably change the stability of

* Corresponding author.
E-mail address: doctorovich@qi.fcen.uba.ar (F. Doctorovich).

0020-1693/$ - see front matter © 2010 Elsevier B.V. All rights reserved.
doi:10.1016/j.ica.2010.10.013

the RSNOs. In a more recent work we presented a complete and detailed experimental characterization and theoretical study of these novel compounds bearing a variety of coordinated nitrosothiols: cysteine derivatives, mercaptosuccinic acid, benzyl thiol and phenyl thiol [13]. Although the free forms of some of these nitrosothiols are extremely unstable and sensitive, upon coordination they become very stable even in aqueous solution. The report of several stable coordinated nitrosothiols which can be isolated as pure materials, allows for a careful study of their decomposition and implies new and interesting intermediates that were not seen before for free RSNOs. Herein we present detailed studies for the decomposition of two coordinated RSNOs with distinct structures and stabilities: *trans*-K[$IrCl_4(CH_3CN)NOSPh$], (**1**) and $K_2[IrCl_5(NOECyS)]$, (**2**) (Fig. 1) supported by MS analysis of the gaseous products, ESI-MS, NMR, UV–Vis spectroscopy, and DFT calculations.

2. Experimental

2.1. Materials

$K_2[IrCl_5NO]$(cysteine-ethyl-ester), *trans*-K[$IrCl_4(CH_3CN)NOSPh$] and their ^{15}N counterparts were made as previously described [13]. $Na^{15}NO_2$ was purchased from Aldrich and used as received.

2.2. UV/Visible spectroscopy and kinetic measurements

Absorption spectra were acquired on a Hewlett-Packard HP8453 diode array spectrometer with 1 cm path length cells, under N_2 preparing the solutions using Schlenk methods. A thermal bath was used to vary temperatures and the solvent was allowed to equilibrate for half an hour prior to use. After the experiment was done the temperature was measured externally. The reaction rates were measured in milliQ water (pH 7, $T = 20–75$ °C, $\lambda = 475–581$ nm) without buffering the solution to avoid secondary reactions with buffer compounds (the pH decreased ca. 2 units during the decomposition). The kinetic rate constants were calculated from the first order plots (ln (Ir-coordinated nitrosothiol concentration) versus time), which in all cases showed $R^2 > 0.99$. The activation parameters were obtained from Eyring plots in the range 300–350 K, with $R^2 = 0.99$ for **1** and 0.98 for **2**, respectively.

In a typical experiment, samples were prepared by placing 0.2–1.2 mg of solid **1** or **2** in a quartz cuvette equipped with a Schlenk adapter and degassing the cuvette. About 3.0 mL degassed milliQ water was placed in another cuvette. Both cuvettes were placed in a water bath to equilibrate to the temperature at which the UV–Vis was to be measured. The cuvette with **1** or **2** was then placed in the UV–Vis spectrometer, with the appropriate temperature maintained by a hot water bath, and the water was added with a syringe. UV–Vis spectra were then measured every 3 min for 3–12 h.

2.3. NMR spectroscopy

The ^1H, ^{13}C, and ^{15}N NMR spectra were obtained at room temperature on a Bruker 500 MHz instrument, with deoxygenated D_2O and DMSO-d_6. ^{15}N NMR spectra were referenced to an external standard of $Na^{15}NO_2$ at 232 ppm. ^1H and ^{15}N NMR spectra were measured by dissolving the compound in degassed deuterated solvent. When measurements were done over a period of time the NMR tubes were stored wrapped in tinfoil to protect from decomposition due to light and the NMR caps were protected with parafilm to minimize the entry of oxygen. In a typical experiment, the decomposition of **1** or **2** were followed in an NMR tube purged with Ar or N_2 and closed with a cap protected with parafilm, by dissolving the corresponding coordinated nitrosothiol in degassed D_2O at r.t. to obtain 0.5 mL of a 0.1 M solution. A first measurement was recorded immediately, and the reaction was followed by taking successive spectra for a period of several days (ca. 1 spectrum per day).

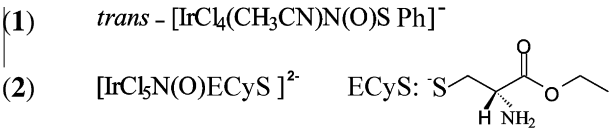

Fig. 1. Structures of the studied iridium coordinated RSNOs.

2.4. Mass spectrometry

2.4.1. Gases

Qualitative and quantitative measurements of the gas production (extracted from the headspace of the reaction mixtures) were conducted using a thermostated homemade flow reactor (volume 0.07 dm^3) linked to a vacuum system and to an Extrel Emba II quadrupolar mass spectrometer through a thin thermostated capillary. The reactor was also supplied with an absolute pressure transducer, MKS Baratron 622 A, and with a mechanical stirrer.

2.4.2. ESI-MS

All fragmentation of the nitrosothiol complexes and the reaction mixtures were performed under exactly the same conditions. Mass spectrometric measurements were performed using a high-resolution hybrid quadrupole (Q) and orthogonal time-of-flight (TOF) mass spectrometer (QTOF from Micromass, UK) operating in the negative ion electrospray ionization mode set from 2100 to 3500 V. Samples dissolved in appropriate anhydrous solvents at room temperature (RT) under an inert atmosphere were injected through an uncoated fused-silica capillary, using a syringe pump (Harvard Apparatus, Pump 11, 15 μL min^{-1}). The temperature of the nebulizer and desolvation gas was set at 100 °C, and the cone voltage was set between 25 and 35 V. Tandem mass spectra (ESI-MS/MS) were acquired using the product ion scan mode via mass selection of the ion of interest, followed by collision-induced dissociation (CID) with Ar using energies varying from 15 to 35 eV with high-accuracy orthogonal TOF mass analysis of the CID ionic fragments. For comparison with experimental data, isotopic patterns were calculated using the MassLynx software.

2.5. Theoretical calculations

All the calculations performed in this work were carried out using the GAUSSIAN 98 [14] package. We have fully optimized the geometries of all species at the pbe1pbe [15] level with sddall basis set without symmetry constraints. Each stationary point in the gas phase was characterized by performing a normal modes analysis. The energetics for the reactions obtained form the pbe1pbe functional with sddall basis set, were validated by single-point energy calculations, using the sddall reference geometries, with the extended SDB-cc-pVDz basis set. The SDB-cc-pVDZ basis set, combines the Dunning cc-p-VDZ basis set [16] on the main group elements with the Stuttgart–Dresden basis set-RECP combination on the transition metals, with an *f*-type polarization exponent [17].

3. Results

3.1. Reaction products and intermediates

When **1** and **2** are allowed to decompose anaerobically in water, in the absence of light, for a period of around 1 week at room tem-

perature (see rate constants below), gases are produced. Almost 50% of the nitrogen from the RSNO is released as N_2 and N_2O when **2** is decomposed in water (Table 1), while **1** produces smaller amounts of gases. Noticeably, very little or no NO is observed, although free RSNOs decompose via homolytic cleavage of the S–NO bond, followed by dimerization to give the corresponding disulfides and NO [18]. Previous mechanisms have explained the presence of N_2 in the decomposition of free RSNOs by means of intramolecular attack from the nitrogen of the cysteine moiety on the nitrosyl group [19]. However, the evolution of N_2 in the decomposition of **1**, where the only activated nitrogen is from the nitrosyl group, indicates that another mechanism is required in order to explain N_2 formation.

The decompositions can also be followed by ^{15}N NMR, by using ^{15}NO labeled **1** and **2**. The starting materials **1** and **2** are seen for the first 1–2 days of the decomposition reaction at 119 and 104 ppm respectively (versus nitromethane), until they disappear. After a few days the presence of coordinated NO^- (bent NO) in both decompositions is observed (Fig. 2A and B, signals at 421 and 428 ppm respectively). This region corresponds only to bent nitrosyl complexes and free RSNOs [20,21]. Free nitrosothiols are not observed [22]. A signal at 141 ppm attributable to NO_2^- was also observed in the case of **1** (free NO_2^- appears at 229 ppm). The signal at 281 ppm could be attributed to a symmetrical bent diazenido (Ir–N=N–Ir). No other species appear in this region of the ^{15}N NMR spectrum, except for nitride and diazenido [21]. In the ^1H NMR spectra, all signals are masked by the starting material and the disulfide products (also observed by ^{13}C NMR, see Supplementary material). No signal was observed in the 10–40 ppm range, indicating that the coordinated NO^- is deprotonated.

The reactions can also be followed by mass spectrometry. The products of the decomposition of **1** and **2** measured by ESI-MS are shown in Table 2. In the case of **1**, coordinated NO_2^-, NO^- (nitroxyl) and $N_3O_2^-$ (or NO^-/N_2O) are identifiable. In the case of **2**, coordinated NO_2^- and cysteine sulfenate ($ECySO^-$) are identifiable. The presence of $[IrCl_3(ECySO)(H_2O)_2]^-$ and $K[IrCl_2(OH)_2(H_2O)NO]^-$ is not only confirmed by analysis of the M^- mass and isotopic pattern, but also by MS–MS, where loss of sulfenic acid and NO respectively are observed (see Supplementary material).

3.2. Kinetic studies

The decomposition of the coordinated RSNOs in water shows first order behavior in coordinated RSNO as shown by both initial rates and plots of the logarithm of concentration versus time. The rate constants and activation parameters are shown in Table 3. The decomposition of **1** is more than 300 times slower than that of free PhSNO. In both cases (**1** and **2**) a negative $\Delta S^{\neq}$ indicates an associative rate-determining step.

3.3. DFT calculations

An energy diagram for the starting materials, observed intermediates and products was obtained for a model complex in the gas phase where the thiol is modeled with methylthiol. Fig. 3 shows that most of the proposed steps are thermodynamically favorable, except for the step of the decomposition of (**a**) to (**b**) plus RSH (Eq. (3)) and the steps that involve the formation of (**f**) (Eq. (8)) and (**f'**) (Eq. (9)). All reactions shown in Fig. 3 are listed below:

$$[IrCl_4(NO)SR]^-(\mathbf{a}) + OH^- + 3H_2O \rightarrow [IrCl_2(NO)(OH)_2]^{2-}\cdot H_2O(\mathbf{c}) + RSOH + 2HCl \quad (1)$$

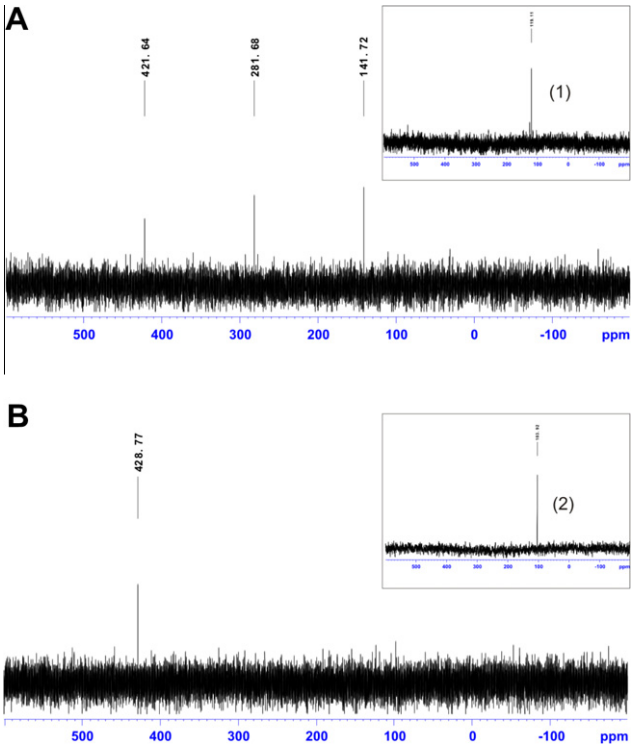

Fig. 2. ^{15}N NMR spectra for the decomposition of **1** (panel A) and **2** (panel B) in water after 1 week at r.t. (anaerobic and in the absence of light). Shifts are relative to nitromethane. The insets in panel A and B show the signals corresponding to **1** and **2** at 119 and 104 ppm respectively.

Table 1
Gases formed by decomposition of coordinated RSNOs in water as measured by MS (headspace analysis).

RSNO	$\%N_2$[a]	$\%N_2O$[a]	%NO[a]
1	7	0.5	4
2	15	34	

[a] Moles of N atoms per 100 moles of RSNO.

Table 2
Soluble decomposition products of iridium coordinated RSNOs in water as measured by ESI-MS.

Compound	Experimental m/z values for MS diagnostic ions (calculated error in ppm)	Intensity (%) relative to base peak[a]
$[IrCl_3(ECySO)(H_2O)_2]^-$	497.9389 (497.9268, 24)	7
$[IrCl_2OH(H_2O)NO_2]^-$	343.9065 (343.9054, 3)	80/6[b]
$K[IrCl_2(OH)_2NO]^-\cdot 2(H_2O)$	401.8933 (401.8874, 15)	30[c]
$[IrCl_3(N_2O)NO]^-$	371.8701 (371.8666, 9)	5[c]

[a] Base peak is $[IrCl_4]^-$ in all cases.
[b] 80% for **1**; 6% for **2**.
[c] Observed for **1** only.

Table 3
Activation enthalpies, entropies, and Gibbs free energies for the decomposition of **1** and **2** in water. All the thermodynamic parameters were determined for the range 293–348 K.

Compound	$\Delta H^{\neq}$ (kcal mol^{-1})	$\Delta S^{\neq}$ (cal mol^{-1} K^{-1})	$\Delta G^{\neq}$ (kcal mol^{-1})	k (s^{-1})
1 (391 nm)	15(1)	−32(3)	24(1)	$7.0 \pm 0.7 \times 10^{-6}$[a]
2 (400 nm)	16(1)	−25(5)	23(2)	$4.4 \pm 0.4 \times 10^{-5}$[a]
PhSNO			21.7 [23]	2.2×10^{-3}[b] [19]

[a] 295 K.
[b] 303 K.

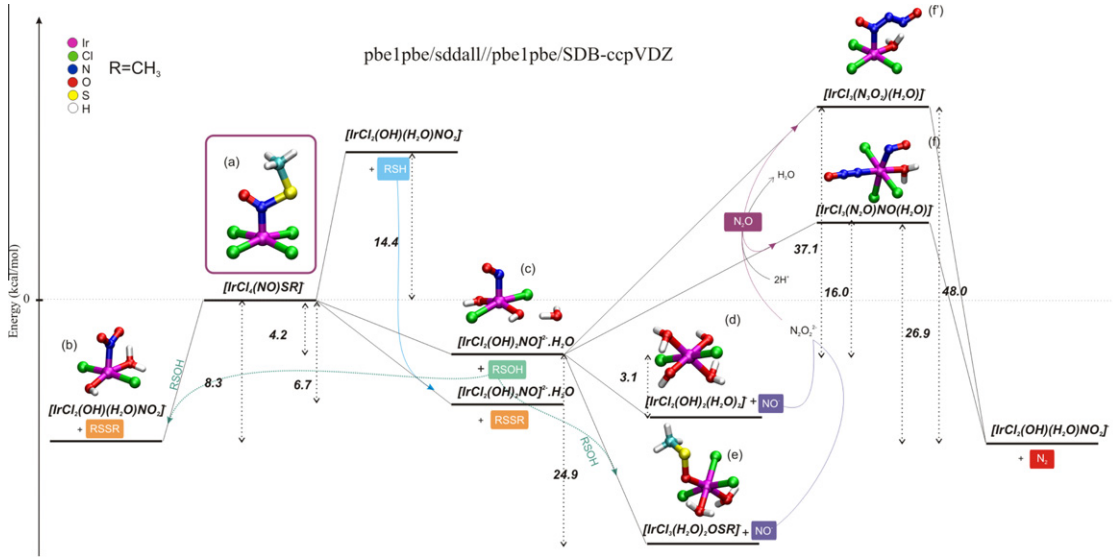

Fig. 3. Calculated energies in gas phase for the proposed steps in the decomposition mechanism.

$$[IrCl_4(NO)SR]^-(\mathbf{a}) + RSOH + 2H_2O \rightarrow [IrCl_2(OH)(H_2O)NO_2]^-(\mathbf{b}) + RSSR + 2HCl \quad (2)$$

$$[IrCl_4(NO)SR]^-(\mathbf{a}) + 3H_2O \rightarrow [IrCl_2(OH)(H_2O)NO_2]^-(\mathbf{b}) + RSH + 2HCl \quad (3)$$

$$[IrCl_4(NO)SR]^-(\mathbf{a}) + RSH + 2H_2O + OH^- \rightarrow [IrCl_2(NO)(OH)_2]^{2-} \cdot H_2O(\mathbf{c}) + RSSR + HCl \quad (4)$$

$$[IrCl_2(NO)(OH)_2]^{2-} \cdot H_2O(\mathbf{c}) + H_2O \rightarrow [IrCl_2(OH)_2(H_2O)_2]^-(\mathbf{d}) + NO^- \quad (5)$$

$$[IrCl_2(NO)(OH)_2]^{2-} \cdot H_2O(\mathbf{c}) + RSOH + HCl \rightarrow [IrCl_3OSR(H_2O)]^-(\mathbf{e}) + NO^- + H_2O \quad (6)$$

$$2HNO^- \rightarrow N_2O_2^{2-} + 2H^+ \rightarrow N_2O + H_2O \quad (7)$$

$$[IrCl_2(NO)(OH)_2]^{2-} \cdot H_2O(\mathbf{c}) + N_2O + HCl \rightarrow [IrCl_3(N_2O)NO(H_2O)]^-(\mathbf{f}) + H_2O + OH^- \quad (8)$$

$$[IrCl_2(NO)(OH)_2]^{2-} \cdot H_2O(\mathbf{c}) + N_2O + HCl \rightarrow [IrCl_3(N_3O_2)(H_2O)]^-(\mathbf{f}') + H_2O + OH^- \quad (9)$$

$$[IrCl_3(N_2O)NO(H_2O)]^-(\mathbf{f}) + H_2O \rightarrow [IrCl_2(OH)(H_2O)NO_2]^-(\mathbf{b}) + N_2 + HCl \quad (10)$$

$$[IrCl_3(N_3O_2)(H_2O)]^-(\mathbf{f}') + H_2O \rightarrow [IrCl_2(OH)(H_2O)NO_2]^-(\mathbf{b}) + N_2 + HCl \quad (11)$$

It is important to mention that N_2O affinity to the iridium complex (**f**) formed (Eq. (8)) is strongly enhanced by the presence of coordinated NO^- (see Supplementary material).

Complexes (**f**) and (**f′**) lead to (**b**) after intramolecular attack (Eqs. (10) and (11)). An intermediate species where N_2 and NO_2^- are coordinated could be formed, as this complex is shown to be quite stable by DFT calculations (see Supplementary material).

4. Discussion

The starting compounds, **1** and **2**, were selected due to their rather dissimilar structures. Accordingly, although both show mostly the same products, the observed relative amounts are noticeably different. While only ca. 12% of gases (based on moles of nitrogen released relative to moles of RSNO) were observed for the decomposition of **1**, almost 50% was observed for **2**, indicating that more products had to be present in the case of **1**. It is therefore not surprising that coordinated NO_2^-, NO^-, and N_2O/NO^- (or $N_3O_2^-$) were observed in solution after the decomposition of **1**, while the decomposition of **2** only showed small amounts of coordinated NO_2^-, NO^-, and sulfenate (compare the 80 versus 6 peak intensity relative to $[IrCl_4]$ for the NO_2^- complex for the decomposition of **1** versus the decomposition of **2** in Table 2, and the absence of NO_2^- and NO^- in the decomposition of **2** in the ESI-MS). The observation of coordinated sulfenate only in the decomposition of **2** and not of **1** could imply that in the case of **1** the sulfenate gets released into solution due to its enhanced lability and once in the free form it rapidly decomposes. It seems reasonable that $PhSO^-$ would be a weaker ligand than the cysteine ethyl ester anion because it has more steric bulk and because the aryl ring stabilizes the negative charge on $PhSO^-$. Therefore, we postulate a first associative step (as confirmed by the kinetic studies), in which H_2O attacks the coordinated RSNO to give an Ir–NO^- complex and the corresponding sulfenic acid (Eq. (1)), which is a known reaction for free RSNOs [24,25] and is energetically favorable (Fig. 3). The ESI-MS results show unequivocally loss of 2 or 3 chlorides which are replaced by H_2O. Chlorides are probably labilized due to the presence of the strongly negative NO^- in the coordination sphere.

In the case of **2**, in which coordinated sulfenate has been observed, we propose as the next step coordination of the sulfenic acid to the iridium center and NO^- release (Eq. (6)), which is also energetically favorable as shown in Fig. 3. The free NO^- protonates at the reaction pH producing nitroxyl (HNO), which rapidly dimerizes to hyponitrite, which decomposes to N_2O under the acidic medium present in these reactions (Eq. (7)). The attack of sulfenic acid to the Ir center in the case of **2**, a ligand displacement reaction, explains the formation of large amounts of gases. In the case of **2**, the coordinating sulfenic acid causes the nitrogen products to dissociate from the iridium center and to be released as gases (for

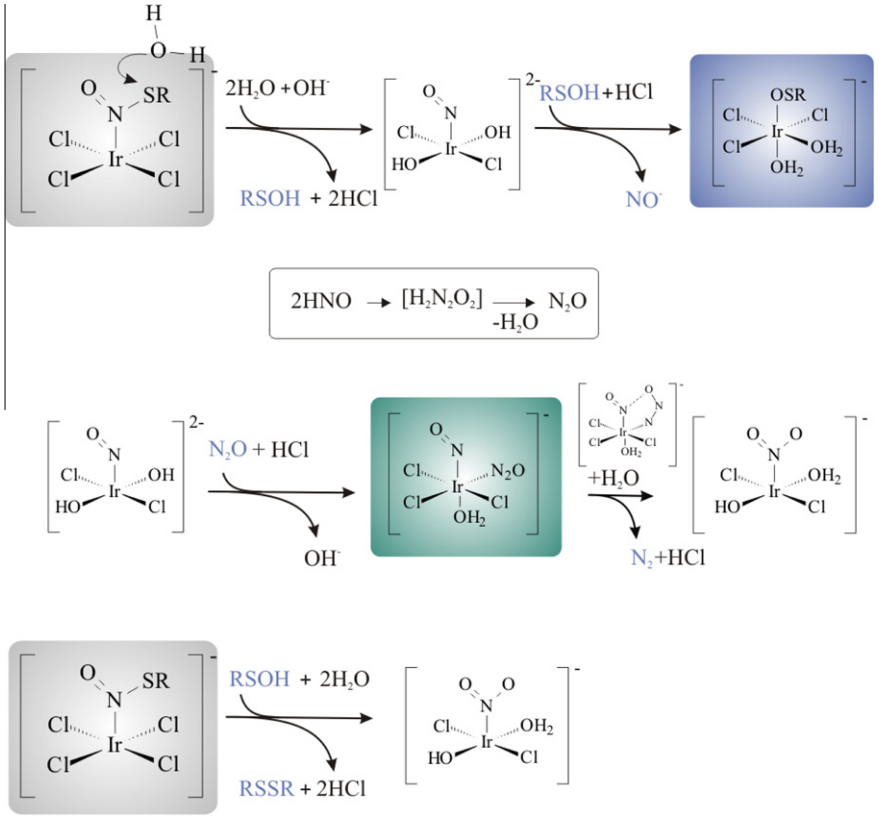

Scheme 1. Proposed mechanism for the decomposition of iridium-coordinated nitrosothiols in water.

example, Eq. (6)). In the decomposition of **1**, the coordinated sulfenic acid is not observed which explains why the nitrogen products are observed in solution, coordinated to the iridium center.

Sulfenic acids are known to react with thiols to produce disulfide (RSSR) [26,27]. Therefore, a competing reaction for free sulfenic acid would be attack to the coordinated RSNO leading to coordinated nitrite and RSSR (Eq. (2)), which is also energetically favorable (Fig. 3). The corresponding disulfides were previously detected as the only final organic decomposition products in the ^{1}H NMR spectra of both complexes (see Supplementary material) [13]. It is also possible that in the decomposition of **1** the first step is formation of NO_2^- and PhSH (Eq. (3)), followed by attack of PhSH to **1**, producing the disulfide and coordinated NO^- (Eq. (4)). However, we tend to disfavor this pathway, since reaction 3 is energetically unfavorable (see Fig. 3).

The conversion of N_2O and NO^- to N_2 and NO_2^- could occur by means of an $N_3O_2^-$ intermediate as has been postulated before [28]. However, the complex $[IrCl_3NO(N_2O)]^-$ could also be formed (Eq. (8)), and although its formation is energetically unfavorable (Fig. 3), after intramolecular attack it may lead to N_2 and coordinated nitrite (Eq. (10)), which leads to energetically favorable (by 26.9 kcal mol^{-1}) products. In principle, at least in the case of **1** part of the N_2 remains coordinated as a bridging diazenido ligand, as observed by ^{15}N NMR. Again, this could be due to the poor coordination abilities of $PhSO^-$, which does not displace N_2 in this case.

A small amount of NO is observed in the case of **1**, and therefore it is possible that NO reacts with HNO (Eq. (12)), which has been described before [29], with a rate constant of $(5.8 \pm 0.4) \times 10^6$ M^{-1} s^{-1}, which ultimately also produces N_2O.

$$HNO + NO \rightarrow N_2O_2^- + H^+ \quad (12)$$

Protons are released during the decomposition, as confirmed by pH measurements showing a decrease of 2–3 units after the reaction, from neutrality up to pH $\approx$ 5.

5. Conclusions

From the above, a mechanism for the decomposition of the coordinated nitrosothiols in water can be postulated (Scheme 1[1]), with a first associative step involving nucleophilic attack of H_2O to the sulfur atom of the coordinated RSNO, producing an NO^- complex and free sulfenic acid, followed by two competing reactions: ligand exchange of this NO^- in the complex with the sulfenic acid (Scheme 1, complex shown in blue), or, to a minor extent, ligand exchange of an OH^- ligand of the NO^- complex with N_2O, to produce an NO^-/N_2O complex (Scheme 1, complex shown in green), which finally renders free N_2 and coordinated NO_2^-. Some of the NO^- is released from the metal center, producing nitroxyl by protonation and finally N_2O by dimerization and loss of H_2O. Finally, for both complexes **1** and **2**, sulfenic acid could react with the starting complex leading to formation of coordinated nitrite and the corresponding disulfide (Scheme 1).

As shown above, the decomposition of coordinated RSNOs occurs through a different mechanism than for free RSNOs, involving the formation of sulfenic acids and the biologically relevant nitroxyl.

Acknowledgments

The authors thank CONICET, UBA (UBACYT X065) and ANPCyT (PICT 2006-2396) for financial support.

Appendix A. Supplementary material

Supplementary data associated with this article can be found, in the online version, at doi:10.1016/j.ica.2010.10.013.

[1] For interpretation of color in Scheme 1, the reader is referred to the web version of this article.

References

[1] P.R. Myers, R.L. Minor, R. Guerra, J.N. Bates, D.G. Harrison, Nature 345 (1990) 161.
[2] H. Al-Sa'Doni, A. Ferro, Clin. Sci. 98 (2000) 507.
[3] D.L.H. Williams, Acc. Chem. Res. 32 (1999) 869.
[4] C. Baciu, K.-B. Cho, J. Phys. Chem. B 109 (2005) 1334.
[5] S. Oae, K. Shinhama, Org. Prep. Proceed. Int. 15 (1983) 165.
[6] K. Szacilowski, Z. Stasicka, Progr. React. Kinet. Mech. 26 (1) (2001) 1.
[7] M.D. Johnson, R.G. Wilkins, Inorg. Chem. 23 (2) (1984) 231.
[8] A.R. Butler, A.M. Calsyharrison, C. Glidewell, P.E. Sorensen, Polyhedron 7 (13) (1988) 1197.
[9] J.D. Schwane, M.T. Ashby, J. Am. Chem. Soc. 124 (2002) 6822.
[10] K. Szacilowski, A. Wanat, A. Barbieri, E. Wasielewska, M. Witko, G. Stochel, Z. Stasicka, New J. Chem. 26 (10) (2002) 1495.
[11] L.L. Perissinotti, D. Estrin, G. Leitus, F. Doctorovich, J. Am. Chem. Soc. 128 (2006) 2512.
[12] F. Doctorovich, F. Di Salvo, Acc. Chem. Res. 40 (2007) 985.
[13] L.L. Perissinotti, G. Leitus, L. Shimon, D.A. Estrin, F. Doctorovich, Inorg. Chem. 47 (2008) 4723.
[14] M.J. Frisch et al., Gaussian 98, Rev. A7, Gaussian Inc., Pittsburgh, PA, 1998 (See Supporting Information for remaining 56 authors).
[15] J.P. Perdew, K. Burke, M. Ernzenof, Phys. Rev. Lett. 77 (1996) 3865.
[16] T.H. Dunning Jr., J. Chem. Phys. 90 (1989) 1007.
[17] J.M.L. Martin, A. Sundermann, J. Chem. Phys. 114 (2001) 3408.
[18] P.G. Wang, M. Xian, X. Tang, X. Wu, Z. Wen, T. Cai, A.J. Janczuk, Chem. Rev. 102 (2002) 1091.
[19] C. Adam, L. García-Río, J.R. Leis, L. Ribeiro, J. Org. Chem. 70 (2005) 6353.
[20] J. Bultitude, L.F. Larkworthy, J. Mason, D.C. Povey, B. Sandell, Inorg. Chem. 23 (1984) 3629.
[21] J. Mason, L.F. Larkworthy, E.A. Moore, Chem. Rev. 102 (2002) 913.
[22] L.L. Perissinotti, A. Turjanski, D.A. Estrin, F. Doctorovich, J. Am. Chem. Soc. 127 (2005) 486.
[23] M.D. Bartberger, J.D. Mannion, S.C. Powell, J.S. Stamler, K.N. Houk, E.J. Toone, J. Am. Chem. Soc. 123 (2001) 8868.
[24] K.G. Reddie, K.S. Carroll, Curr. Opin. Chem. Biol. 12 (2008) 746.
[25] L. Tao, M. English, Biochemistry 43 (2004) 4028.
[26] F.A. Davis, R.H. Jenkins Jr., S.Q.A. Rizvi, S.G. Yocklovich, J. Org. Chem. 46 (1981) 3467.
[27] P. Nagy, M.T. Ashby, J. Am. Chem. Soc. 129 (2007) 14082.
[28] J.L. Moruzzi, J.T. Dakin, J. Chem. Phys. 49 (1968) 5000.
[29] V. Shafirovich, S.V. Lymar, Proc. Natl. Acad. Sci. 99 (2002) 7340.